Supporting Information

Stabilization of the ring-opened Rhodamine probe via multi-noncovalent interactions for dual-mode detection of nitazenes

Yujie Feng,[a] Yudong Li, *[b] Bingbing Zhao,[a] Chuanfang Zhao,[b] Jingxiang Li,[b] Luyan Yang,[2] Baiyi Zu *[bc] and Xincun Dou *[abc]

[a]Department of Physics Science and Technology, Xinjiang University, Urumqi 830046, China

[b]Xinjiang Key Laboratory of Trace Chemical Substances Sensing, Xinjiang Technical Institute of Physics and Chemistry, Chinese Academy of Sciences, Urumqi 830011, China

[c]Center of Materials Science and Optoelectronics Engineering, University of Chinese Academy of Sciences, Beijing 100049, China

Corresponding Author: *Yudong Li: liyd@ms.xjb.ac.cn *Baiyi Zu: byzu@ms.xjb.ac.cn *Xincun Dou: xcdou@ms.xjb.ac.cn

Table of contents

1. Experimental Section

1.1 Synthesis Process of RhB-I

The RhB-I probe was prepared following a modified procedure based on a previously reported method[1]. RhB-I was synthesized via a one-step condensation reaction between Rhodamine B and hydrazine hydrate. Rhodamine B (2.4 g, 5 mmol) was dissolved in 60 mL of absolute ethanol in a round-bottom flask. Subsequently, 10 mL of hydrazine hydrate was added dropwise, and the mixture was refluxed for 16 hours. The color of the reaction mixture changed from dark pink to transparent orange. The reaction mixture was cooled to room temperature, and the ethanol was completely removed using rotary evaporation. Excess hydrazine hydrate was eliminated by washing with 1 M HCl; 1 M NaOH was then added with continuous stirring until the solution pH reached 8-9. The pale orange precipitate was filtered and washed with deionized water to afford a light pink compound with a yield of 85%. ^{1}H NMR (400 MHz, DMSO-d_6) δ 7.79-7.73 (m, 1H), 7.51-7.42 (m, 2H), 7.00-6.95 (m, 1H), 6.38 (s, 2H), 6.33 (d, J = 1.4 Hz, 4H), 4.26 (s, 2H), 3.31 (q, J = 7.1 Hz, 8H), 1.08 (t, J = 6.9 Hz, 12H). ^{13}C NMR (100 MHz, DMSO-d_6) δ 165.7, 153.5, 152.3, 148.6, 132.8, 130.1, 128.6, 128.1, 123.9, 122.6, 108.2, 105.9, 97.9, 65.2, 44.1, 12.9. **HRMS (ESI)** calcd for $C_{28}H_{33}N_4O_2$ m/z $[M+H]^+$: 457.2598; found: 457.2598.

1.2 Synthesis Process of RhB-II

The RhB-II probe was prepared following a modified procedure based on a previously reported method[2]. Ethylenediamine (1.0 mL, 15.08 mmol) was added dropwise to a solution of Rhodamine B (1.0 g, 2.08 mmol) in 25 mL of ethanol. The solution was heated to reflux for 16 h and evaporated to dryness under reduced pressure. The resulting residue was dissolved in water and extracted with DCM (2 × 15 mL). The combined organic phases were washed with water and dried over anhydrous Na_2SO_4. The solvent was removed via rotary evaporation, and the remaining solid was dried in vacuo, affording a pinkish powder (yield of 85%). ^{1}H NMR (400 MHz, Chloroform-*d*) δ 7.92-7.86 (m, 1H), 7.45-7.41 (m, 1H), 7.10-7.06 (m, 1H), 6.44 (s, 1H), 6.41 (s, 1H), 6.37 (d, J = 2.6 Hz, 2H), 6.28-6.25 (m, 2H), 3.32 (q, J = 7.2 Hz, 8H), 3.18 (t, J = 6.6 Hz, 2H), 2.41 (t, J = 6.6 Hz, 2H), 1.41 (s, 2H), 1.15 (t, J = 7.0 Hz, 12H). ^{13}C NMR (100 MHz, Chloroform-*d*) δ 168.6, 153.5, 153.3, 148.8, 132.4, 131.2, 128.7, 128.0, 123.8, 122.7, 108.1, 105.6, 97.7, 64.9, 44.3, 43.8, 40.8, 12.6. **HRMS (ESI)** calcd for $C_{30}H_{37}N_4O_2$ m/z $[M+H]^+$: 485.2911; found: 485.2911.

1.3 Synthesis Process of RhB-III

The RhB-III probe was prepared following a modified procedure based on a previously reported method[3]. Rhodamine B (1.20 g, 2.5 mmol) was dissolved in ethanol (30 mL). An excess of 1,3-propanediamine (2 mL) was added dropwise to the solution, and the mixture was refluxed for 12 h. The solution was concentrated via rotary evaporation. Water (20 mL) was added to the resulting mixture, and the aqueous layer was extracted with DCM (2×20 mL). The combined organic phases were washed twice with water and dried over anhydrous sodium sulfate. The solvent was removed via rotary evaporation, and the residue was dried under vacuum to afford a pale pink solid with a yield of 70%. ^{1}H NMR (400 MHz, Chloroform-*d*) δ 7.88 (s, 1H), 7.44 (s, 2H), 7.08 (s, 1H), 6.42-6.24 (m, 6H), 3.33 (q, J = 7.5 Hz, 8H), 3.21 (s, 2H), 2.50 (t, J = 6.6 Hz, 2H), 2.33 (s, 2H), 1.25 (s, 2H), 1.16 (t, J =

7.0 Hz, 12H). ^{13}C NMR (100 MHz, Chloroform-*d*) δ 168.4, 153.5, 153.3, 148.8, 132.3, 131.2, 128.8, 128.0, 123.8, 122.7, 108.0, 105.6, 97.7, 65.0, 44.3, 38.9, 36.9, 31.2, 12.6. **HRMS (ESI)** calcd for $C_{31}H_{39}N_4O_2$ m/z $[M+H]^+$: 499.3068; found: 499.3068.

2. Testing Process

2.1 Preparation of the etonitazene solution

The concentration of etonitazene standard stock solution was 1 mg/mL and the solvent was MeOH. Then the stock solutions were diluted with MeOH to obtain various concentrations of etonitazene solutions.

2.2 Optimization of solvent type of the probe

The RhB-I probe was dissolved in various solvents (ACN, DMF, DMSO, THF, 1,4-dioxane, and NMP) to form 0.37 mg/mL solutions, and fluorescence images and spectra were recorded. Then, 10 μL of 1 mg/mL etonitazene solution was mixed with 190 μL of the above probe solutions. After completion of the reaction, fluorescence and absorbance spectra were recorded. The settings of the fluorescence spectra measurements were λ_{ex}= 365 nm, slits: 1.5 nm; λ_{em}= 520 nm, slits: 1.5 nm.

2.3 Optimization of the probe's concentration

RhB-I solutions of different concentrations (0.2, 0.4, 0.6, 0.8, 1, 2, 3 mM in ACN) were prepared. Then, 190 μL of each probe solution was mixed with 10 μL of 50 μg/mL etonitazene. After the reaction, the fluorescence images and spectra were recorded with a setting of λ_{ex} = 365 nm, slits = 1.5 nm, λ_{em} =520 nm, slits = 1.5 nm.

2.4 Optical responses of the three probes toward etonitazene

Three probes (RhB-I, RhB-II and RhB-III) were dissolved in ACN to form 0.37 mg/mL solutions, respectively. Then, 10 μL of 50 μg/mL etonitazene in MeOH was added to 190 μL of the probe solution. Before measurement, the optimal excitation wavelength for the three probes was confirmed, and fluorescence spectra before and after addition of etonitazene were recorded.

Note: The probe concentration was maintained at 0.37 mg/mL for all experiments. All the optical images were recorded with a mobile phone of HUAWEI Mate 60 RS under natural light and 365 nm illumination. All fluorescent spectra were obtained by spectrometer (λ_{ex}= 365 nm, slits: 1.5 nm; λ_{em}= 520 nm, slits: 1.5 nm, Edinburgh FLS1000), with error bars indicating the standard deviation from three independent experiments.

2.5 Sensitivity study

The concentration of etonitazene stock solution was 50 μg/mL, then, it was diluted as a series of 0.5, 2.5, 5, 10, 15, 20, 25, 30, 35, 40, and 45 μg/mL. The above diluted etonitazene solution (10 μL) was mixed with 0.37 mg/mL probe solution (190 μL) for the detection reaction. The fluorescence images and spectra were recorded with a setting of λ_{ex}= 365 nm, slits = 1.5 nm; λ_{em}= 520 nm, slits = 1.5 nm.

2.6 Specificity study

Twenty-two potential interferents were selected to evaluate the specific recognition ability of the probe toward etonitazene, including structural analogs (e.g., indole, indazole, 3,4-dimethyl-1H-pyrazole, benzimidazole), coexisting substances (e.g., fentanyl, diazepam, bromazolam, etomidate), and other drugs (e.g., opium, methamphetamine, cocaine, heroin, synthetic cannabinoids). All interferents were prepared in MeOH at a concentration of 2 mg/mL. Then, 5 μL of 1 mg/mL etonitazene and 5 μL of 2 mg/mL interferent was mixed with 190 μL of 0.37 mg/mL probe solution, respectively, and fluorescence images and spectra were recorded at λ_{ex} = 365 nm, slits = 1.5 nm; λ_{em} = 520 nm, slits = 1.5 nm.

2.7 Anti-interference study

5 μL of 1 mg/mL etonitazene and 5 μL of 2 mg/mL each potential interferent were mixed at a 1:1 ratio (V/V). Then, 10 μL of the mixture was added to a cuvette containing 190 μL of 0.37 mg/mL RhB-I probe solution. After incubation, fluorescence images and spectra were recorded at λ_{ex} = 365 nm, slits = 1.5 nm, λ_{em} = 520 nm, slits = 1.5 nm.

2.8 pH study

First, different pH solutions (pH 1, 2, 3, 4, 5, 6, 7, 8, 9, 10, 11, 12, 13, and 14) were prepared using ultrapure water. Then, a series of 1:1 mixtures were prepared by mixing 10 μL of etonitazene with 10 μL of each pH solution. Then, 20 μL of each mixture was added to 180 μL of the RhB-I probe solution (0.37 mg/mL). After incubation, fluorescence images and spectra were recorded at λ_{ex} = 365 nm, slits = 1.5 nm, λ_{em} = 520 nm, slits = 1.5 nm.

3 Preparation and Testing of the Probe-loaded Porous Polymer-based Device

3.1 Preparation of probe-loaded porous polymer-based sensing units

The functionalized polyurethane substrate was cut into cuboids of 3 × 3 × 3 mm, immersed in the RhB-I fluorescent probe solution (0.8 mM) for 2 min, and then stored at room temperature for subsequent testing.

3.2 Detection of etonitazene using Drugs Analyst

The 20 μL aliquot of each analyte sample was precisely deposited onto the cells of the sensing chip, followed by insertion of the chip into our self-developed Drugs Analyst for automated result output.

3.3 Testing of the RhB-I-based sensing chip to etonitazene with different concentrations

Etonitazene methanol solutions with concentrations of 0, 0.01, 0.05, 0.1, 0.2, 0.3, 0.4, 0.5, 0.6, 0.7, 0.8, 0.9, and 1 mg/mL were first prepared. Then, 20 μL of the above etonitazene solution was added onto the RhB-I-functionalized substrate, and the corresponding optical images were recorded using an industrial camera.

3.4 Preparation of simulated real-sample interferents

10 μL of 1 mg/mL etonitazene and 10 μL of interfering substances (including saliva, e-liquid, blood, urine, and hair, were mixed at a 1:1 ratio (V/V). Then, 20 μL of the mixture was dropped onto the polyurethane substrate. Subsequently, the Drug Analyst was used for detection.

4 Calculation Details

To insight into the mechanism of Rhodamine-based probe toward nitazene substances, computational studies were carried out. The structures of probes, the ring-opening reaction transition states, intermediates, etonitazene, and probe-etonitazene complexes were optimized with PBE1PBE-D3(BJ)/def2svp method and polarizable continuum model (PCM) solvation model [4-10]. Besides, frequency analyses were performed with the same method to verify that all the reactants, intermediates, and complex structures have no imaginary frequency, and all the transition state structures possess only one imaginary frequency. To study the non-covalent interactions between probes and etonitazene, independent gradient model (IGM) and atoms-in-molecules (AIM) analyses were carried out with Multiwfn software[11-15]. To explore the mechanism of probe sensing etonitazene, the excited states of probes and probe/etonitazene complexes were optimized and frequency analyzed with TD-PBE1PBE-D3(BJ)/def2svp method[16, 17]. Then, the electron-hole analyses were carried out with Multiwfn software[18]. Note that all the computations were carried out with Gaussian16 software[19], and the images were obtained through VMD software based on the outputs of Multiwfn[20].

5 Figures

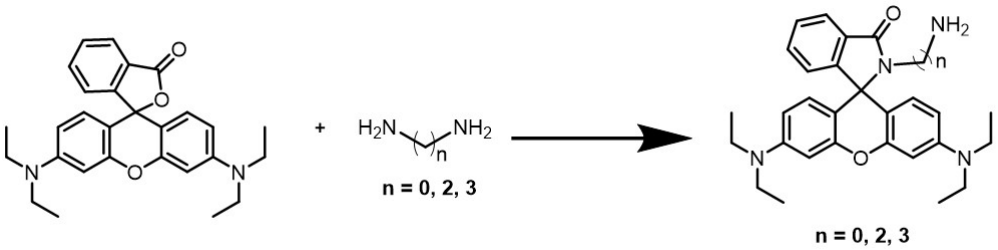

Figure S1. Synthetic procedures for RhB-I, RhB-II and RhB-III probes.

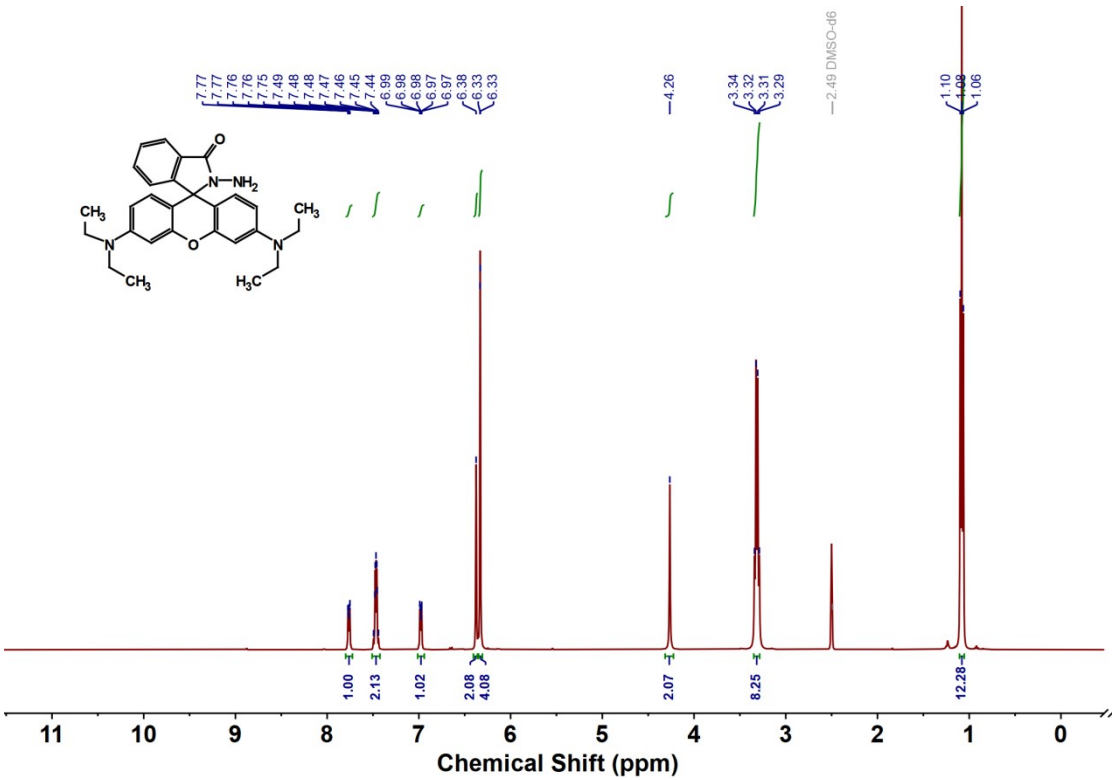

Figure S2. ^{1}H NMR spectrum of RhB-I.

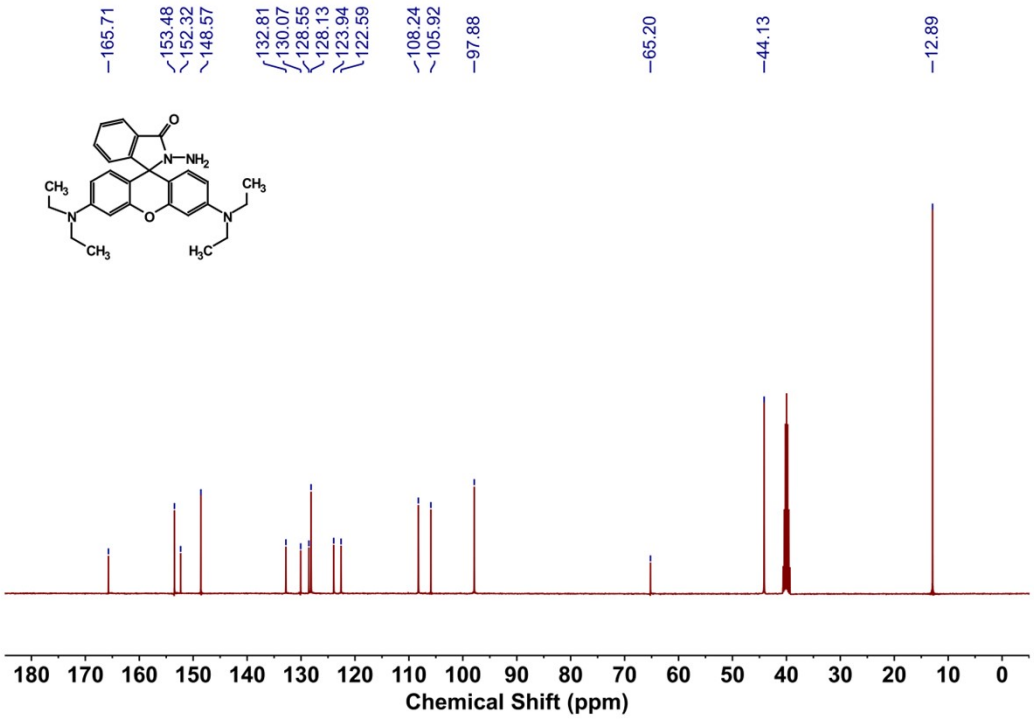

Figure S3. ^{13}C NMR spectrum of RhB-I.

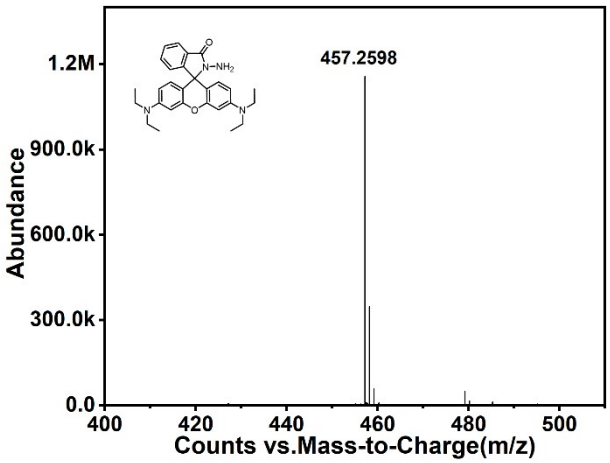

Figure S4. HRMS spectrum of RhB-I.

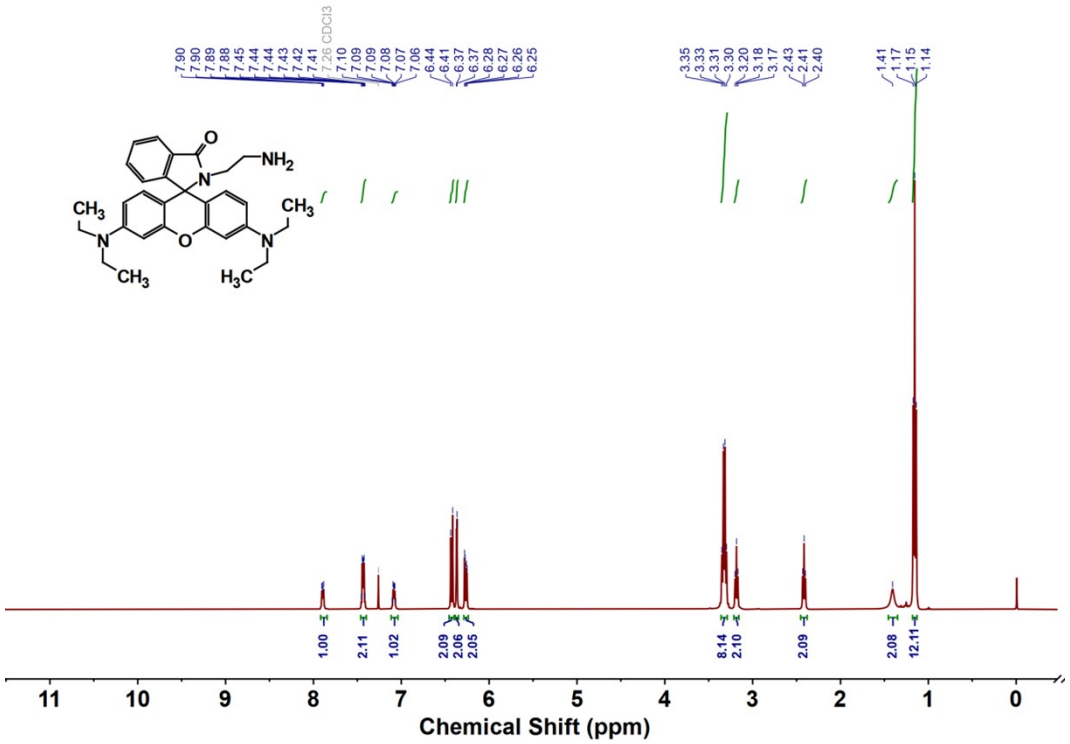

Figure S5. ^{1}H NMR spectrum of RhB-II.

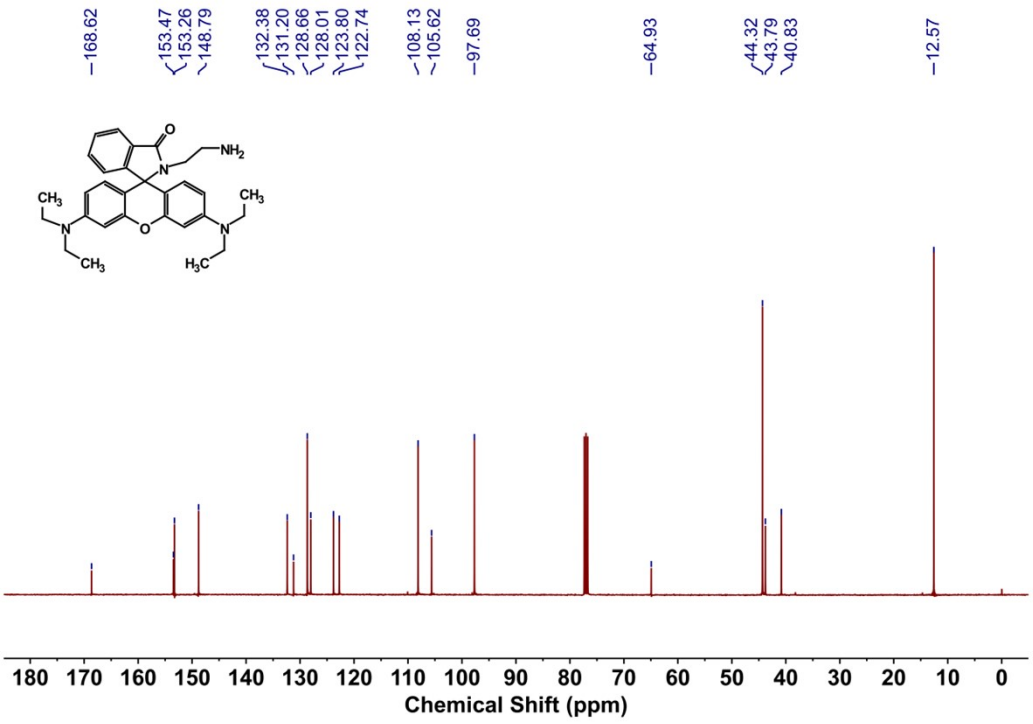

Figure S6. ^{13}C NMR spectrum of RhB-II.

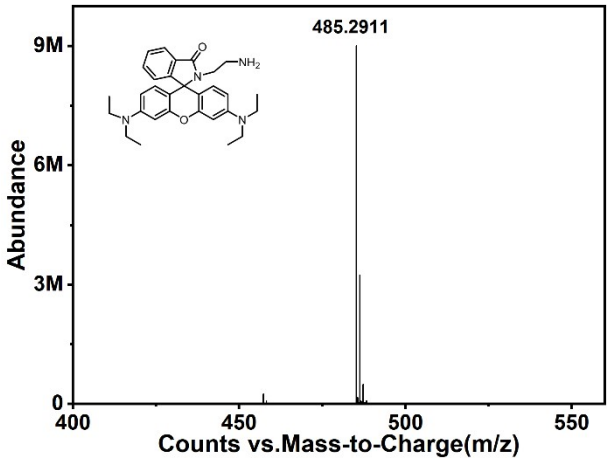

Figure S7. HRMS spectrum of RhB-II.

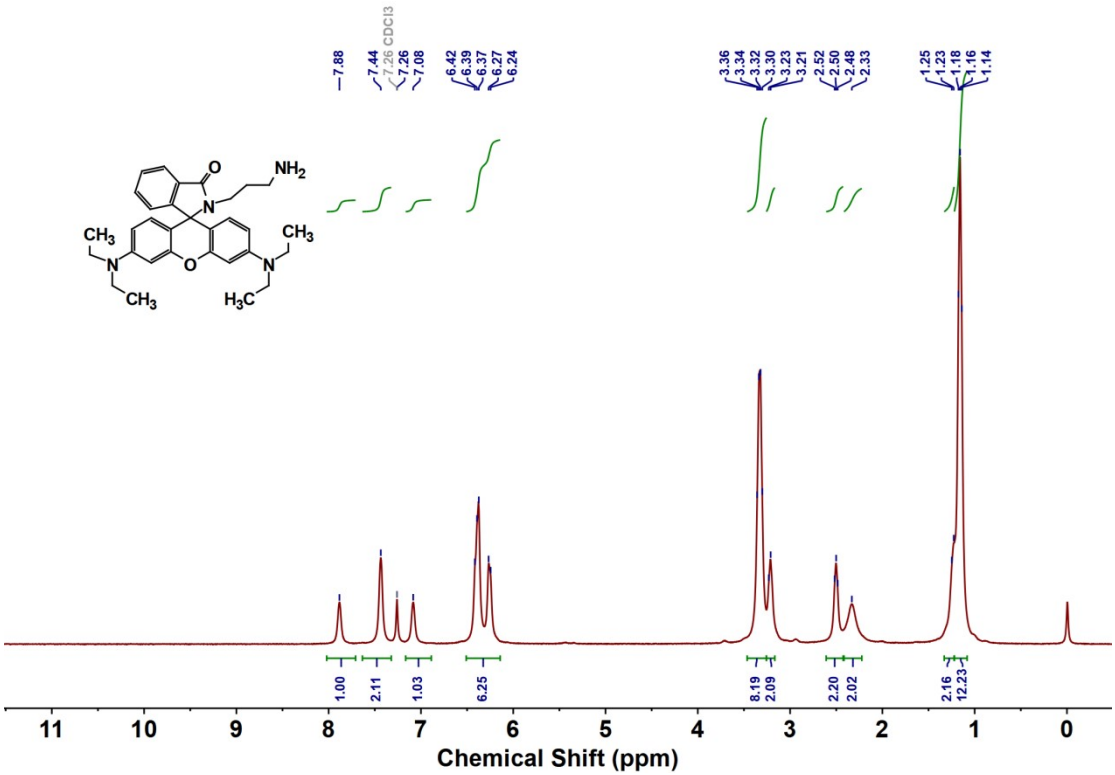

Figure S8. ^{1}H NMR spectrum of RhB-III.

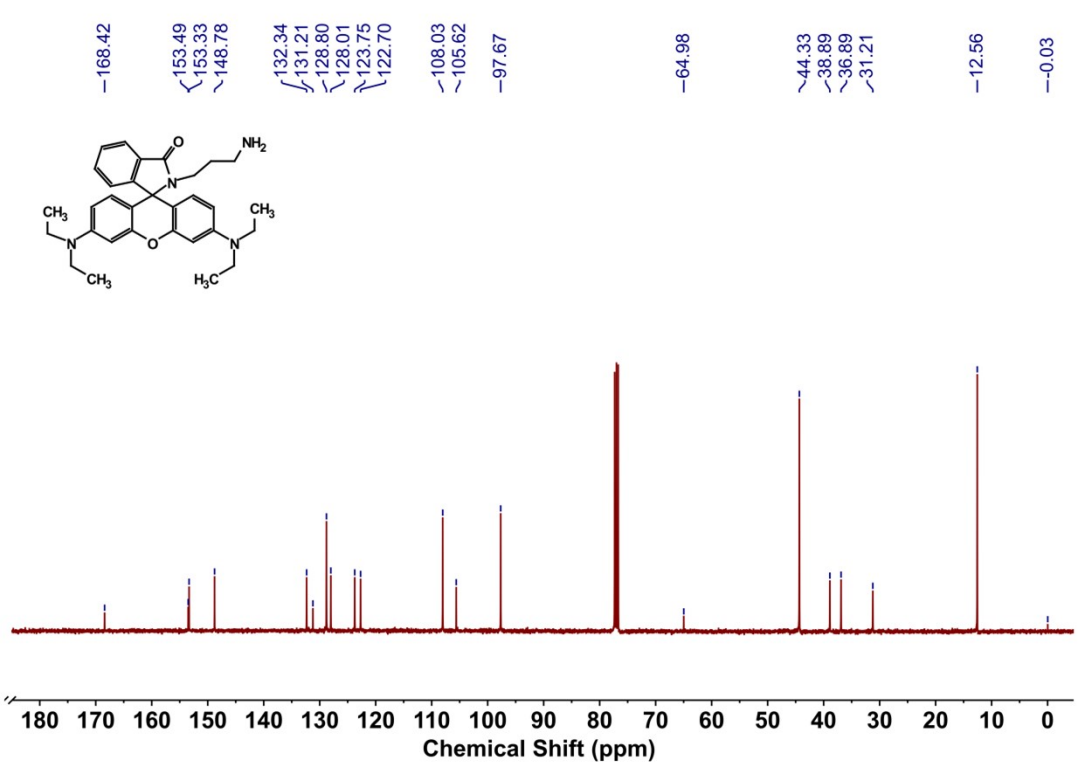

Figure S9. ^{13}C NMR spectrum of RhB-III.

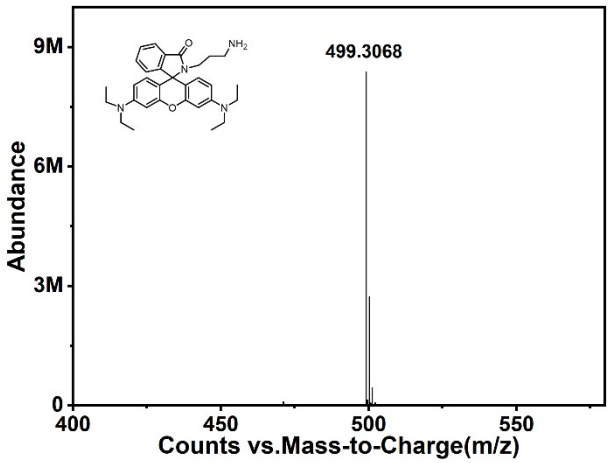

Figure S10. HRMS spectrum of RhB-III.

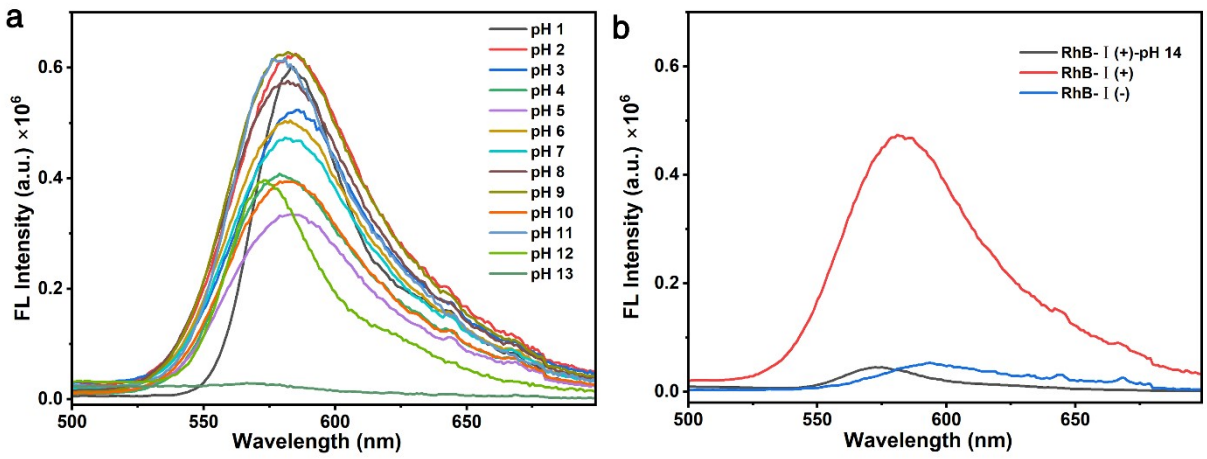

Figure S11. (a) Fluorescence spectra of the RhB-I probe at various pH values, (b) fluorescence quenching of RhB-etonitazene complex *via* strong base.

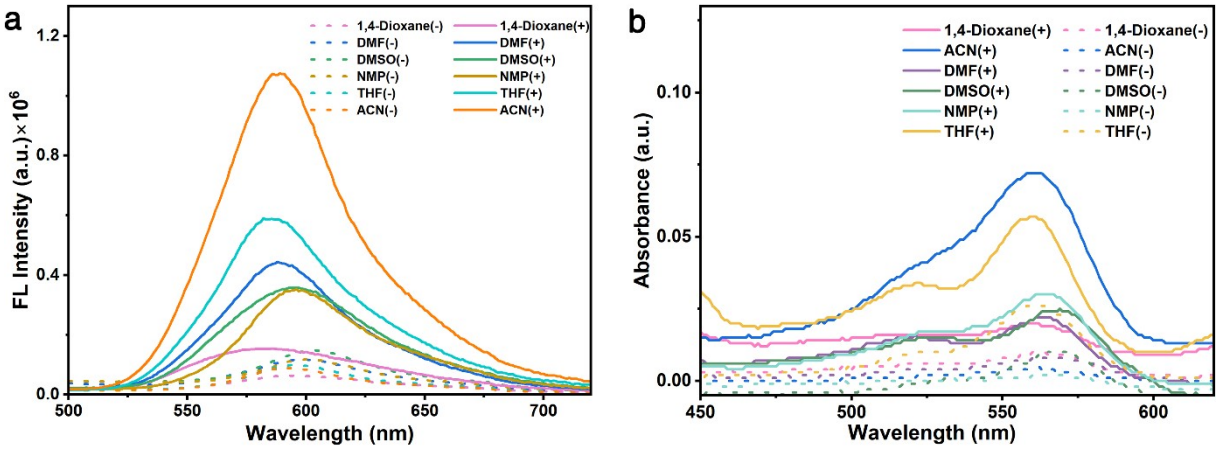

Figure S12. Optimization of solvent types: (a) fluorescence spectra and (b) UV-Vis absorption spectra of the probe before and after the addition of etonitazene.

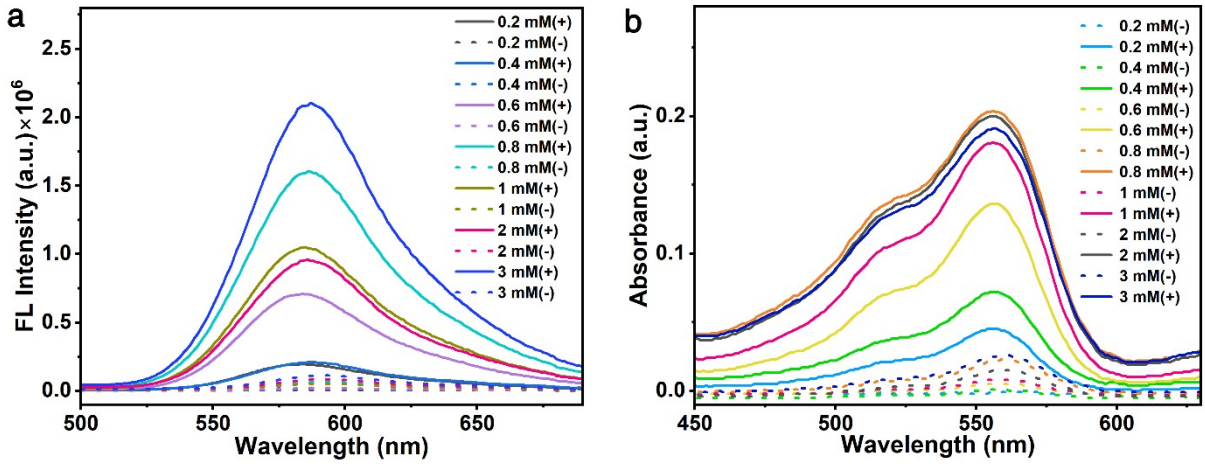

Figure S13. Optimization of the probe concentration: (a) fluorescence spectra, and (b) absorption spectra before and after detecting etonitazene.

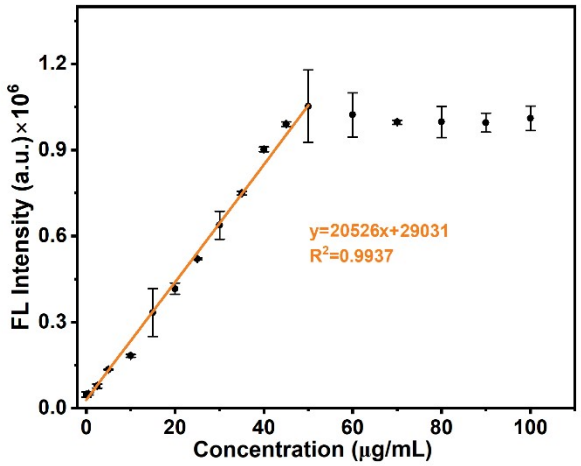

Figure S14. Correlation between the emission intensity at 585 nm and the concentration of etonitazene.

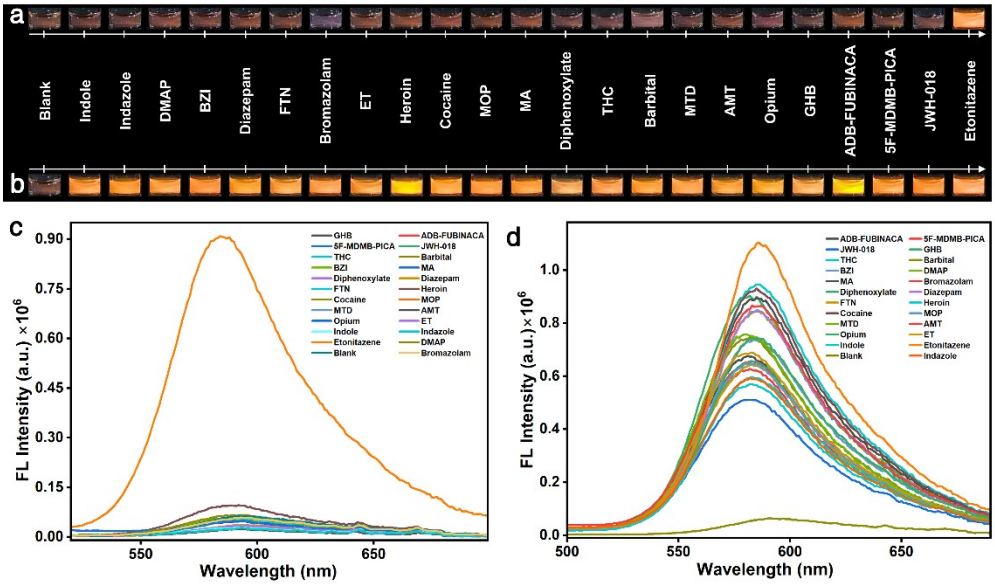

Figure S15. Specificity and anti-interference study of the probes towards etonitazene: (a) optical images for specificity evaluation, (b) optical images for anti-interference evaluation, and (c, d) the corresponding fluorescence spectra.

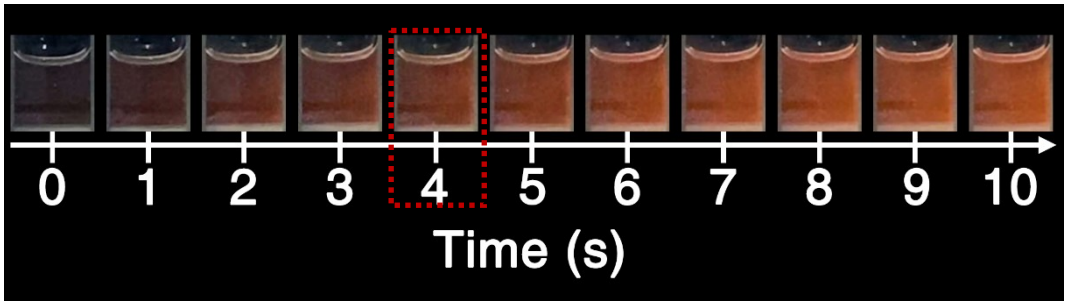

Figure S16. The response time of the RhB-I probe toward etonitazene.

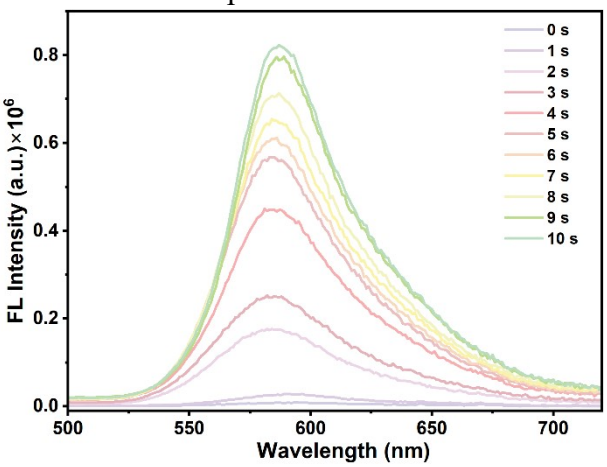

Figure S17. Time-dependent fluorescence spectra of the RhB-I probe upon addition of etonitazene.

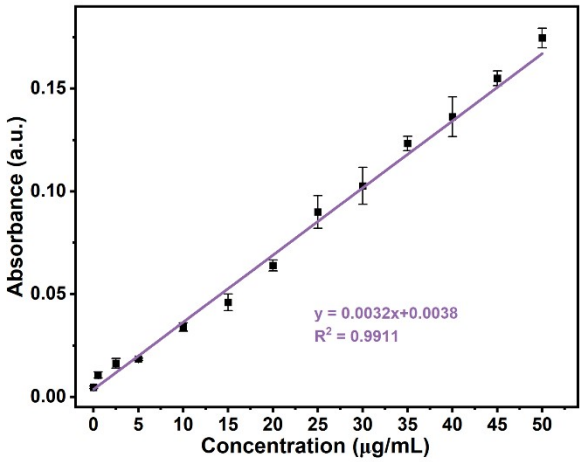

Figure S18. Correlation between the absorbance intensity at 556 nm and the concentration of etonitazene.

Figure S19. Specificity and anti-interference study of the probes towards etonitazene: (a) optical images for specificity evaluation, (b) optical images for anti-interference evaluation, and (c, d) the corresponding absorbance spectra.

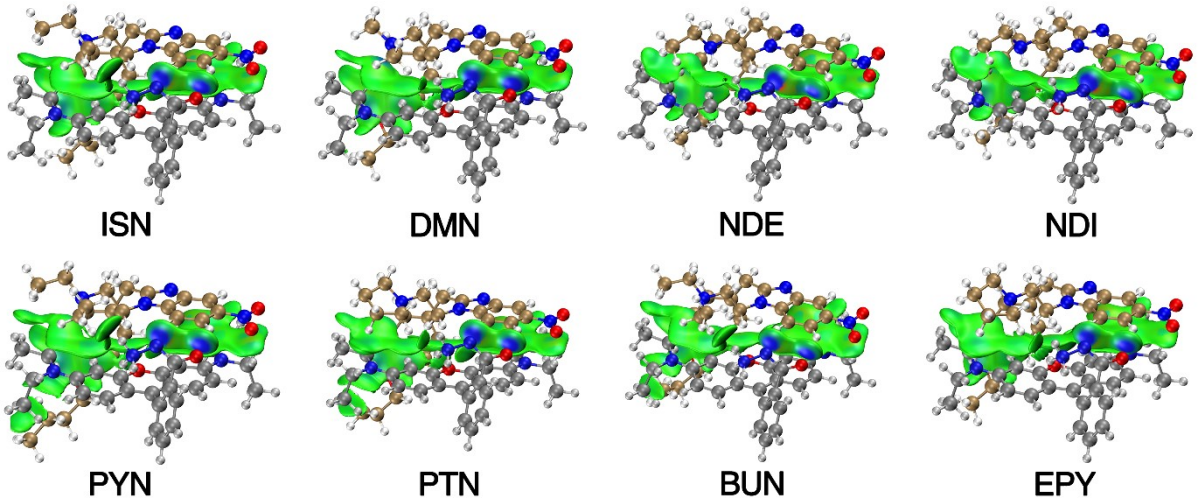

Figure S20. The intermolecular interaction analysis of the RhB-I complexes with various nitazenes (ISN, DMN, NDE, NDI, PYN, PTN, BUN, and EPY).

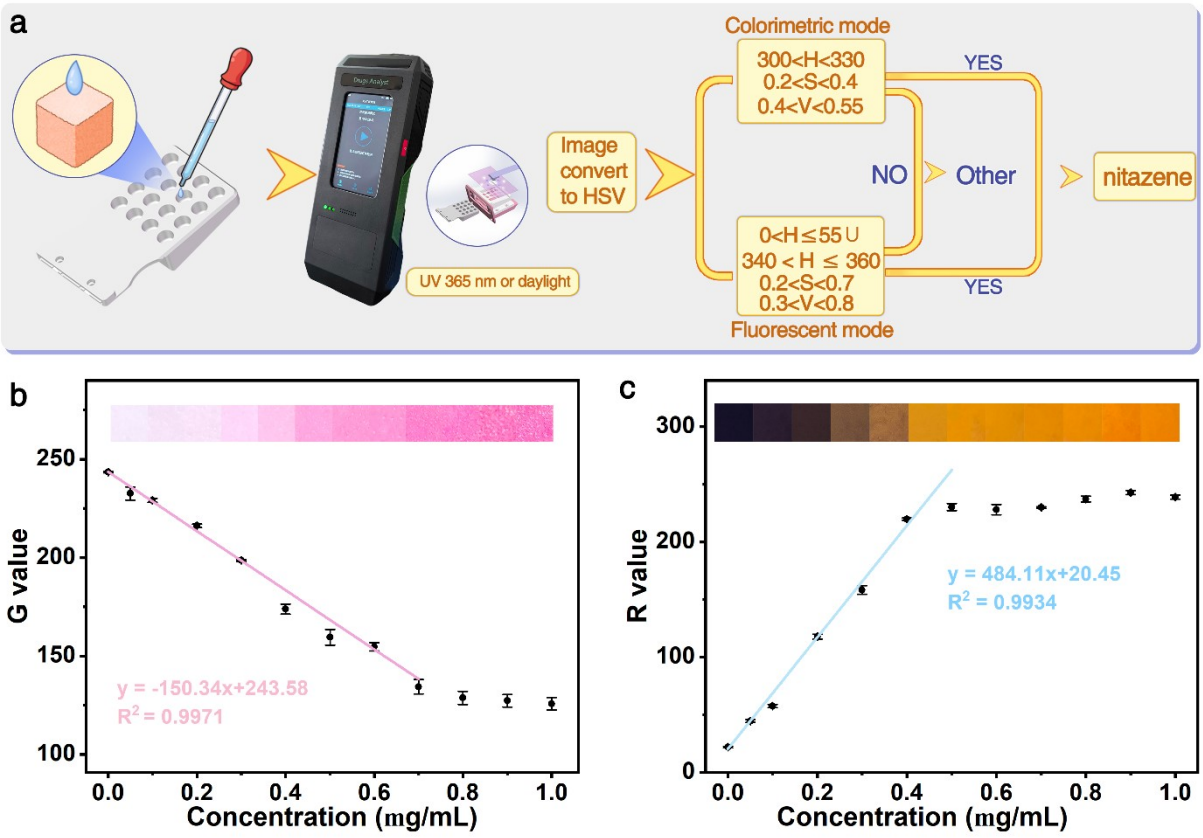

Figure S21. (a) Schematic illustration of the Drugs Analyst for the qualitative discrimination of etonitazene. (b) Corresponding correlation between the analyte concentration and the G value extracted from colormetric images, and (c) correlation between the analyte concentration and the R value extracted from fluorescence images.

6 Tables

Table S1. Relative energy between the probe RhB-I/RhB-II with etonitazene.

Analysis object	Etonitazene (Hartree)	Probe (react) (Hartree)	Probe (TS1) (Hartree)	Probe (IN1) (Hartree)	Probe/ Etonitazene (Hartree)
RhB-I	-1299.37	-1455.61	-1455.55	-1455.58	-2754.99
RhB-II	-1299.37	-1534.23	-1534.15	-1534.17	-2833.58

Analysis object	Probe (react) (kcal/mol)	Probe (TS1) (kcal/mol)	Probe (IN1) (kcal/mol)	Probe/Etonitazene (kcal/mol)
RhB-I	0	34.37	15.99	-8.22
RhB-II	0	47.37	36.19	11.21

Table S2. Comparison of the main sensing performance for synthetic nitazene detection based on recently developed analytical methods and this work.

Detection method	Type of test	Linear range	Theoretical detection limit	Actual detection limits	Response time	Ref.
GC-EI-MS	nitazene	/	/	5-10 ppm	/	21
DART-TD-MS	nitazene	/	/	/	/	22
UHPLC-MS/MS	Isotonitazene	0.05 - 10.0 ng/mL	0.015 ng/mL	/	/	23
NMR	protonitazene	/	/	/	/	24
LC-MS/MS	nitazene	0.5 - 50 ng/mL	/	0.5 ng/mL	/	25
FT-IR	nitazene	/	/	/	/	26
Fluorescent and Colorimetric	**nitazene**	**0 - 50 µg/mL**	**1.9 ng/mL and 483 ng/mL**	**2.5 µg/mL and 5 µg/mL**	**4 s**	**This work**

7 References

1 S. Sarkar, A. Chatterjee, K. Ghosh, N. N. Ghosh, A. Dutta, A. Kumar, A. K. Mandal, K. Biswas, *New Journal of Chemistry,* 2025, **49**, 10991-11000.

2 C. Wende, N. Kulak, *Chemical Communications,* 2015, **51**, 12395-12398.

3 X. Zhang, S. Sumiya, Y. Shiraishi, T. Hirai, *Journal of Photochemistry and Photobiology A: Chemistry,* 2009, **205**, 215-220.

4 C. Adamo, V. Barone, *The Journal of chemical physics,* 1999, **110**, 6158-6170.

5 J. P. Perdew, K. Burke, M. Ernzerhof, *Phys Rev Lett,* 1996, **77**, 3865-3868.

6 S. N. Maximoff, M. Ernzerhof, G. E. Scuseria, *The Journal of chemical physics,* 2004, **120**, 2105-2109.

7 F. Weigend, R. Ahlrichs, *Physical chemistry chemical physics : PCCP,* 2005, **7**, 3297-3305.

8 T. Brinck, A. G. Larsen, K. M. Madsen, K. Daasbjerg, *The journal of physical chemistry. B,* 2000, **104**, 9887-9893.

9 S. Miertuš, E. Scrocco, J. Tomasi, *Chem Phys,* 1981, **55**, 117-129.

10 S. Grimme, S. Ehrlich, L. Goerigk, *J Comput Chem,* 2011, **32**, 1456-1465.

11 C. Lefebvre, G. Rubez, H. Khartabil, J. C. Boisson, J. Contreras-Garcia, E. Henon, *Physical chemistry chemical physics : PCCP,* 2017, **19**, 17928-17936.

12 S. Emamian, T. Lu, H. Kruse, H. Emamian, *J Comput Chem,* 2019, **40**, 2868-2881.

13 T. Lu, F. Chen, *J Comput Chem,* 2012, **33**, 580-592.

14 T. Lu, *The Journal of chemical physics,* 2024, **161**, 082503.

15 T. Lu, *Angew Chem Int Ed Engl,* 2025, **64**, e202504895.

16 E. Runge, E. K. U. Gross, *Physical Review Letters,* 1984, **52**, 997-1000.

17 A. Dreuw, M. Head-Gordon, *Chem Rev,* 2005, **105**, 4009-4037.

18 Z. Liu, T. Lu, Q. Chen, *Carbon,* 2020, **165**, 461-467.

19 M.J. Frisch, G.W. Trucks, H.B. Schlegel, G.E. Scuseria, M.A. Robb, J.R. Cheeseman, G. Scalmani, V. Barone, G.A. Petersson, H. Nakatsuji, X. Li, M. Caricato, A.V. Marenich, J. Bloino, B.G. Janesko, R. Gomperts, B. Mennucci, H.P. Hratchian, J.V. Ortiz, A.F. Izmaylov, J.L. Sonnenberg, Williams, F. Ding, F. Lipparini, F. Egidi, J. Goings, B. Peng, A. Petrone, T. Henderson, D. Ranasinghe, V.G. Zakrzewski, J. Gao, N. Rega, G. Zheng, W. Liang, M. Hada, M. Ehara, K. Toyota, R. Fukuda, J. Hasegawa, M. Ishida, T. Nakajima, Y. Honda, O. Kitao, H. Nakai, T. Vreven, K. Throssell, Jr.J.A. Montgomery, J.E. Peralta, F. Ogliaro, M.J. Bearpark, J.J. Heyd, E.N. Brothers, K.N. Kudin, V.N. Staroverov, T.A. Keith, R. Kobayashi, J. Normand, K. Raghavachari, A.P. Rendell, J.C. Burant, S.S. Iyengar, J. Tomasi, M. Cossi, J.M. Millam, M. Klene, C. Adamo, R. Cammi, J.W. Ochterski, R.L. Martin, K. Morokuma, O. Farkas, J.B. Foresman and D.J. Fox, Gaussian 16 Rev. C.01. Wallingford, CT. 2016.

20 W. Humphrey, A. Dalke, K. Schulten, *J Mol Graph,* 1996, **14**, 33-38.

21 C. Phelps, E. K. Hardwick, A. N. Couch, J. T. Davidson, *Journal of Forensic Sciences,* 2025, **70**, 1949-1962.

22 M. M. Vandeputte, K. Van Uytfanghe, N. K. Layle, D. M. St. Germaine, D. M. Iula, C. P. Stove, *ACS Chemical Neuroscience,* 2021, **12**, 1241-1251.

23 F. Mueller, C. Bogdal, B. Pfeiffer, L. Andrello, A. Ceschi, A. Thomas, E. Grata, *Forensic Science International,* 2021, **320**, 110686.

24 R. Mandrioli, M. Protti, R. Di Lecce, L. Mercolini, *Journal of Chromatography Open,* 2026, **9**, 100305.

25 A. L. Pacana, B. N. Skillman, *Journal of Analytical Toxicology,* 2025, **49**, 520-528.

26 M. M. Kimani, S. Kern, A. Lanzarotta, M. Thatcher, L. M. Lorenz, S. W. Smith, M. Collins, G. W. Howe, A. E. Wetherby, *Drug Testing and Analysis,* 2023, **15**, 539-550.